Are Long-Chain Alkanes Hydrophilic?

Robin Underwood, Jill Tomlinson-Phillips, and Dor Ben-Amotz*

Purdue University, Department of Chemistry, 560 Oval Drive, West Lafayette, Indiana 47907

Received: December 22, 2009; Revised Manuscript Received: May 15, 2010

Although short *n*-alkane chains are classic examples of hydrophobic solutes, mounting evidence points to a hydrophilic crossover for the hydration free energies (ΔG) of sufficiently long *n*-alkane chains. Experimental and simulation results for the hydration of *n*-alkanes from methane (C1) to docosane (C22) are combined with fundamental thermodynamic relations to elucidate intermolecular contributions to ΔG. Theoretical bounds on the influence of solute conformation on ΔG are inferred by considering the hydration of idealized linear (all-trans) and globular (spherical) model solutes. More detailed theoretical extrapolations of experimental and simulation results imply that the water-mediated free energy change associated with collapsing an all-trans C100 chain is on the order of −100 kJ/mol and thus that *n*-alkane chains of this length and longer may be hydrophilic ($\Delta G < 0$).

1. Introduction

The diversity of chemical processes in Earth's biosphere is linked to the ubiquity and versatility of water in facilitating complex chemical processes, such as the formation of micelles and membranes, as well as protein folding and binding reactions. Understanding such processes requires developing an accurate description of the free energy driving forces which guide biological and other water-mediated interactions, spanning molecular to macromolecular length scales.[1] Here, we focus specifically on the role water plays in the collapse of nonpolar, *n*-alkane chains of various lengths. While short *n*-alkanes remain largely extended when dissolved in water,[2] long alkanes are expected to collapse to a globular structure whose hydration free energy (ΔG) is lower than that of an extended alkane chain. If the latter decrease in ΔG is large enough, then we find that a crossover from hydrophobic ($\Delta G > 0$) to hydrophilic ($\Delta G < 0$) hydration is predicted to occur for long chains. Although this work pertains only to *n*-alkane chains, one might also expect such length scale dependent changes in water-mediated interactions to influence the equilibrium structures and aggregation properties of other synthetic and biological macromolecules.

In his seminal 1959 article on protein denaturation, Walter Kauzmann stated that "*the hydrophobic bond is probably one of the more important factors involved in stabilizing the folded conformation in many native proteins*".[3] Kauzmann's "hydrophobic bond" arises from the water-mediated free energy driving force to aggregate nonpolar groups in water. These ideas have motivated numerous subsequent studies of polymer collapse and protein folding[4−12] as well as the recent interest in nanoscale hydrophobicity.[13−17]

Recent simulations by Ferguson, Debenedetti, and Panagiotopoulos have led to the surprising conclusion that water plays little or no role in determining the hydrated conformations of *n*-alkane chains up to C22.[2] On the other hand, other simulations of *n*-alkanes up to C100[18] and model flexible bead−spring polymers comparable to C25 and C50[9,12] suggest that water-mediated interactions may play a more significant role in driving the collapse of longer nonpolar chains. More specifically, the simulations of Goel, Athawale, Garde, and Truskett imply that the water-mediated free energy driving force to fold a C25 chain is about −30 kJ/mol and for a C50 chain is about −65 kJ/mol, respectively.[12] If the water-mediated folding free energy continued to be approximately proportional to chain length, then the hydration free energy of a collapsed C100 *n*-alkane chain would be more than −100 kJ/mol below that of an extended C100 chain. We shall see that a water-mediated driving force of this magnitude is consistent with additional independent theoretical estimates described in this work. What is surprising, and has apparently not been previously recognized, is that these predictions also point to the existence of a hydrophilic crossover, which implies *n*-alkanes longer than about C100 have negative rather than positive hydration free energies.

Although early experimental measurements[19−22] erroneously implied a hydrophilic crossover at around C18, subsequent experimental measurements by Tolls et al. up to C15,[23] as well as the recent Ferguson et al. simulations up to C22,[2] suggest that no such crossing occurs at these chain lengths, but leave open the possibility that a hydrophilic crossover may occur at longer chain lengths. The existence of such a hydrophilic crossover may appear at first glance to be inconsistent with the fact that the surface tension of a macroscopic oil−water interface is positive, implying that large oil drops should have a positive hydration free energy. However, our results indicate that the surface tension associated with the interface between water and a collapsed polymeric *n*-alkane chain may in fact be negative. This counterintuitive prediction can most simply be understood as resulting from the fact that the density of methyl groups at the latter interface is significantly higher than at a macroscopic oil−water interface. Thus, the van der Waals cohesive interaction energy between water and a collapsed long-chain alkane (per unit interfacial area) is expected to be substantially more negative than that at a macroscopic oil−water interface.

The remainder of this article begins, in Section 2, by clarifying the connection between ΔG, hydropathy, and water-mediated contributions to chain folding. Then, in Section 3, experimental, simulation, and theoretical results are combined to predict ΔG values for all-trans (rigid) and flexible chains and to compare the effective surface tensions of hydrated *n*-alkanes and macroscopic aqueous interfaces. In Section 4, we summarize

* Corresponding author. E-mail: bendor@purdue.edu. Phone: (765) 434-5256.

10.1021/jp912089q
Published on Web 06/16/2010

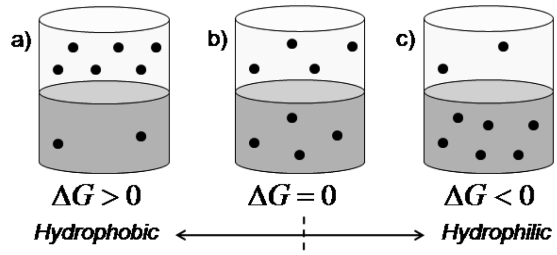

Figure 1. Hydropathy of a solute is determined by the sign of its hydration free energy ΔG, which in turn reflects the ratio of the equilibrium concentrations of the solute in the vapor and aqueous phase ρ_{vap}/ρ_{aq} (see eq 1).

and discuss the close connection between water-mediated chain collapse and the conjectured hydrophilic crossover, and also explain why the existence of such a hydrophilic crossover is not incompatible with the low solubility of solid paraffins.

2. Hydropathy and Hydration Free Energies

Water-mediated processes are often characterized by a delicate interplay of hydrophobic and hydrophilic interactions.[24,25] Although numerous hydrophobicity (or hydropathy) scales have been proposed, none are unique or universally accepted.[26] In this work, we relate hydropathy directly to the sign of a solute's hydration free energy ΔG. More specifically, we obtain ΔG from an Ostwald solvation process in which a dilute gas of solute molecules is allowed to equilibrate with liquid water, as illustrated in Figure 1. Thus, ρ_{aq} and ρ_{vap} represent the equilibrium number densities (concentrations) of the solute in the aqueous and vapor phases, respectively, and $K_{hyd} = \rho_{aq}/\rho_{vap}$ is the associated hydration equilibrium constant from which ΔG is obtained.[27]

$$\Delta G = -RT \ln K_{hyd} = -RT \ln\left(\frac{\rho_{aq}}{\rho_{vap}}\right) \quad (1)$$

A molecular statistical mechanical analysis of hydration further reveals the explicit connection between ΔG and intermolecular solute−water interactions. More specifically, the Widom potential distribution theorem (in its inverse form) leads to the following expression for ΔG (where R is the gas constant and T is the absolute temperature).[28−30]

$$\Delta G = RT \ln\langle e^{\Psi/RT}\rangle = \langle\Psi\rangle + RT \ln\langle e^{\delta\Psi/RT}\rangle \equiv E_{uv} - TS_{uv} \quad (2)$$

The solute−water interaction energy in a particular solvent conformation is Ψ, and $\delta\Psi = \Psi - \langle\Psi\rangle$ reflects instantaneous fluctuations in Ψ from its mean value, where $\langle ... \rangle$ represents the canonical average of all configurations of the equilibrium solution (at the same temperature and average pressure as the system of interest).[28] Thus, E_{uv} represents the average solute−solvent (uv) potential energy of interaction, including both repulsive (packing) and attractive (dispersive and electrostatic) contributions. Similarly, S_{uv}, as defined by eq 2, reflects the entropic contribution to ΔG arising from solute−solvent energy fluctuations. Note that E_{uv} is not equivalent to the corresponding hydration energy (either at constant pressure or constant volume), as the latter quantities contain an additional contribution arising from the change in the water−water interaction energy induced by the solute.[29,30]

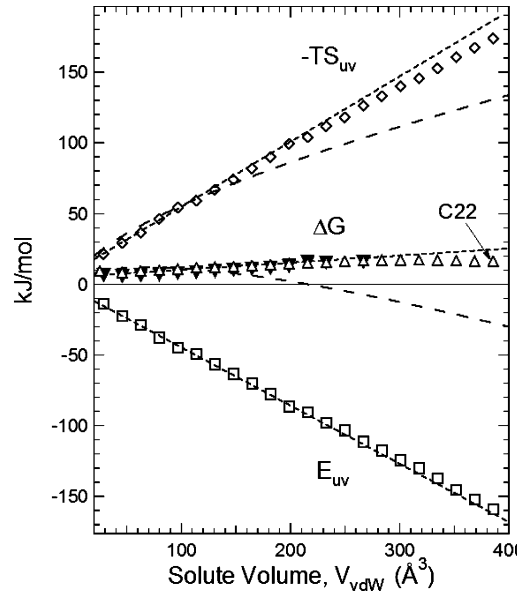

Figure 2. Experimental[23,32] (closed markers) and simulation[2] (open markers) results for the hydration free energies ΔG of n-alkanes, as well as the corresponding energetic E_{uv} and entropic $-TS_{uv}$ contributions (see eq 2), plotted against van der Waals volumes for n-alkanes C1−C22. The theoretical bounds obtained for idealized all-trans and spherical solutes are indicated by short and long dashed curves, respectively.

In Figure 2, we compare E_{uv}, $-TS_{uv}$, and ΔG values of n-alkanes (points) with theoretical bounds (dashed curves, generated as described in Section 3) for the hydration of the n-alkanes methane (C1) to docosane (C22), plotted against their molecular van der Waals volumes (as further described in the Appendix).[31] The experimental ΔG values (solid inverted triangles) of n-alkanes up to C15 were determined using eq 1, from liquid solubility and/or vapor pressure measurements.[23,32] Beyond this chain length, no reliable experimental measurements are available. However, the recent n-alkane ΔG simulations of Ferguson et al. (open triangle points)[2] are in excellent agreement with experimental results and extend up to C22.

In this work, we treat the Ferguson et al. ΔG results[2] as the best currently available estimates of the experimental ΔG values up to C22. To determine the E_{uv} values of n-alkanes (open squares, in Figure 2), we have performed independent simulations of hydrated n-alkanes using OPLS-AA/TIP4P potential functions (as further described in the Appendix). Note that the OPLS-AA/TIP4P potential functions have previously been shown to accurately predict the global hydration thermodynamics (ΔG, ΔH, and ΔS) of linear, branched, and cyclic alkanes up to C6[33] and are thus expected to produce reliable E_{uv} values for n-alkanes. Because S_{uv} is difficult to explicitly determine using numerical computer simulations, the $-TS_{uv}$ values (open diamonds) in Figure 2 are inferred from E_{uv} and ΔG using eq 2 ($TS_{uv} = E_{uv} - \Delta G$).

The results shown in Figure 2 indicate that the small, positive ΔG values of short n-alkanes derive from a positive entropic penalty, $-TS_{uv}$, arising primarily from the formation of a cavity having the same size and shape as the solute, and a negative interaction energy, E_{uv}, arising primarily from van der Waals (dispersive) alkane-water interactions. Both E_{uv} and S_{uv} may in general depend on the size and shape of the solute, as well as on its electronic structure and its conformational flexibility. Thus, the value of ΔG is dictated by a delicate balance of opposing E_{uv} and $-TS_{uv}$ contributions, as illustrated in Figure 2.

3. Evidence for a Hydrophilic Crossover

The dashed curves in Figure 2 represent theoretical bounds pertaining to idealized all-trans (short-dashed lines) and perfectly spherical (long-dashed curves) alkane-like solutes. The upper (all-trans) theoretical bound on ΔG was obtained by extrapolating experimental results for short *n*-alkane chains (from C1 to C6). Since these short-chain *n*-alkanes are primarily extended when dissolved in water,[2] their incremental change in ΔG per methyl group may be used to predict the ΔG values of all-trans *n*-alkanes of any length. The corresponding E_{uv} values were obtained from simulation measurements for hydrated flexible chains (open markers) and linear all-trans chains (lower dashed line), and the corresponding $-TS_{uv}$ values were inferred using eq 2. The idealized, spherical solute bound (long dashed curves) was obtained using $-TS_{uv}$ for hard spheres of the same volume as the corresponding *n*-alkane,[34] combined with simulated E_{uv} values of flexible *n*-alkane chains (open squares). (Note that the latter ΔG values represent a lower bound to the true ΔG values of tightly folded globular chains, as the E_{uv} values of such chains are expected to be smaller, less negative, than those of equilibrated flexible chains.) Although the latter spherical solute bound undergoes a hydrophilic crossover (from positive to negative ΔG values) at $V_{vdW} \sim 200$ Å^3, this crossover volume is expected to be smaller than the crossover volume of flexible *n*-alkane chains, whose shapes are certainly neither perfectly spherical nor perfectly extended (all-trans). This expectation is clearly consistent with the experimental and simulation ΔG values in Figure 2, which reflect the fact that the equilibrium structures of flexible *n*-alkane chains have solvent excluded volumes (and surface areas) which are intermediates between the idealized all-trans and spherical limits.

The difference between the all-trans bound and flexible chain ΔG values provides a measure of the water-mediated free energy driving force to fold *n*-alkane chains from an all-trans conformation. For example, the small difference between the all-trans (short-dashed curve) and flexible (open triangles) ΔG predictions for C22 implies a water-mediated folding free energy of about -10 kJ/mol. However, in spite of this small driving force for folding, Ferguson et al. found that there was very little difference between the conformational distributions of C22 chains in the vapor and aqueous phases, as C22 chains folded into very similar semiglobular conformations in both phases.

In general, the existence of a hydrophilic crossover is dictated by the way in which both TS_{uv} and E_{uv} depend on the shape of the solute. Our simulation results suggest that the magnitude of E_{uv} decreases as an *n*-alkane chain folds but does so in such a way that chains of the same exposed surface area (SASA) have approximately the same E_{uv}. Although such a simple correlation between E_{uv} and SASA has been found to break down for proteins,[35] our results suggest that it is reasonable for *n*-alkanes up to C100 (as further discussed below and shown in Figure 4). The values of TS_{uv} have a somewhat different dependence on solute shape and so are not the same for solutes of the same SASA. However, the TS_{uv} and E_{uv} values are well correlated to each other for *n*-alkanes up to C22, as shown in Figure 3.

Although the correlation shown in Figure 3 is approximately linear, it has a slight negative curvature. Note that eq 2 indicates that a strictly linear correlation between TS_{uv} and E_{uv} would also imply a linear dependence of ΔG on *n*-alkane chain length, while the experimental and simulation results shown in Figure 2 indicate that ΔG is a nonlinear function of chain length. Thus, a quadratic relationship between TS_{uv} and E_{uv} is the lowest-order nonlinear correlation which is consistent with the chain

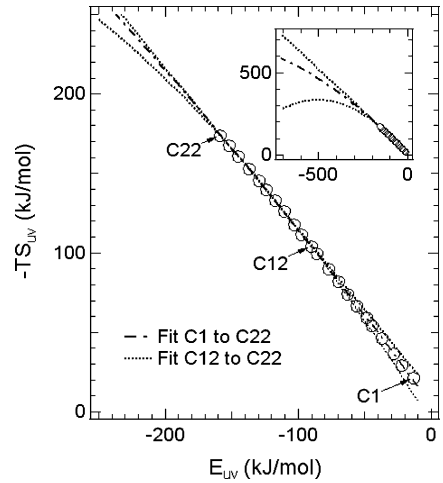

Figure 3. The E_{uv} and $-TS_{uv}$ values of *n*-alkanes C1−C22 (points) are found to be well correlated with each other. The curves represent a quadratic fit through all the points (dot-dashed) and linear and quadratic fits through C12−C22 points (dotted curves). Extrapolations of the latter curves to chain lengths on the order of C100 are shown in the inset panel and used to estimate the $-TS_{uv}$ values of long *n*-alkanes from simulated E_{uv} values (as shown in Figure 4 and further described in the text).

length dependence of ΔG. The dot-dashed curve in Figure 3 is a quadratic fit to all of the points (C1−C22), while the two dotted curves represent linear and quadratic fits to the longer chain points (C12−C22). The fact that the curvature is negative implies that ΔG decreases with chain length for long *n*-alkanes and thus may change sign (and become negative) for sufficiently long chains.

Extrapolation of the correlation between TS_{uv} and E_{uv} to chain lengths much longer than C22 clearly becomes increasingly uncertain, as illustrated by the inset in Figure 3, which shows how the three fits to the short chain results diverge with increasing chain length. Nevertheless, the observation that ΔG for any chain length arises from two largely compensating intermolecular (TS_{uv} and E_{uv}) contributions suggests that such extrapolations may be used to provide physically reasonable estimates of ΔG for long alkanes, as illustrated in Figure 4. The dot-dashed curves in Figure 4 represent TS_{uv} and ΔG predictions obtained using the correlation indicated by the dot-dashed curve in Figure 3. These predictions are obtained by making use of our simulation results, which indicated that both linear and globular *n*-alkanes of the same SASA have approximately the same E_{uv} values, represented by the lower dashed line in Figure 4. This correlation between E_{uv} and SASA, combined with that between TS_{uv} and E_{uv} (shown in Figure 3), is used to obtain the dot-dashed curves in Figure 4. Note that these ΔG predictions imply that folded, equilibrium configurations of *n*-alkane chains with SASA values greater than about 15 nm^3 will be hydrophilic, which corresponds to a chain length near (but somewhat below) C100.

The SASA and E_{uv} values of globular C100 chains were obtained by hydrating a variety of collapsed chain conformations (as described in the Appendix). The resulting SASA and E_{uv} values are indicated by the open circles in Figure 4, each of which pertains to a particular globular C100 conformation. Note that these globular conformations all have SASA values that are much smaller than an extended (all-trans) C100 chain, indicated by the solid point in Figure 4. The TS_{uv} and ΔG values of these various globular C100 chains are again predicted using the quadratic correlation (solid curve) in Figure 3. The error bars on the ΔG points represent the range of predictions obtained

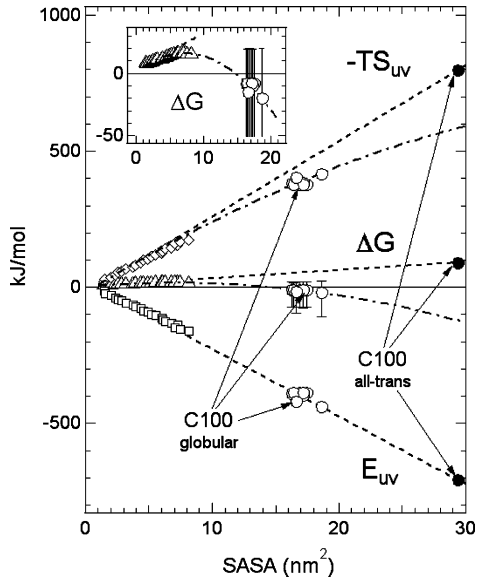

Figure 4. Hydration free energies ΔG (and the associated E_{uv} and $-TS_{uv}$ values) for *n*-alkanes C1−C22 (points) and the corresponding all-trans and collapsed *n*-alkane results (curves) are displayed as functions of the solute's excluded surface area (SASA). The solid points on the dashed curves (with SASA $\sim$ 30 nm^2) represent all-trans C100 values. The cluster of open circular points (with SASA $\sim$ 17 nm^2) pertain to collapsed C100 chain conformations, obtained by combining simulated E_{uv} values with the correlations in Figure 3 (as further described in the text). The inset shows an expanded view of ΔG vs SASA, which better illustrates the relationship between the maximum in ΔG and the C100 results.

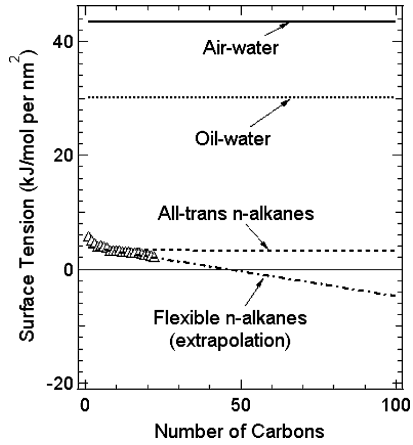

Figure 5. Macroscopic air−water and oil−water surface tensions are compared with the apparent molecular surface tensions of rigid (all-trans) and flexible *n*-alkanes (see text for further details).

using the two dotted curve correlations in Figure 3. Note that the upper limit corresponds to assuming a linear dependence of ΔG on chain length, which is inconsistent with the observed curvature of ΔG. Thus, the physically reasonable values of ΔG for a globular C100 chain are expected to lie below the upper error bars and thus to be negative (or perhaps very near zero), as indicated by the open circle ΔG points and lower error bars (obtained using the C12−C22 quadratic TS_{uv} vs E_{uv} correlation in Figure 3).

The above predictions that long-chain alkanes are hydrophilic may at first glance appear to conflict with the positive experimental value for the macroscopic oil−water interfacial surface tension.[36] However, this apparent conflict is not inconsistent with our hydrophobic crossover predictions, as the effective densities of methyl groups at the two interfaces are expected to be quite different. More specifically, the average density of methyl groups at a macroscopic oil−water interface is approximately equal to the average methyl group density in a liquid alkane, which is of the order of 30 $\pm$ 3 (carbons/nm^3) for liquid *n*-hexane to *n*-dodecane, while the methyl group density in a collapsed C100 chain (estimated using the molecular volume of the collapsed chain and the fact that it contains 100 methyl groups) implies a density that is approximately twice as large. Thus, one expects the cohesive (dispersive) interaction between water and a collapsed *n*-alkane chain to be significantly larger (more negative) than at a macroscopic oil−water interface. This expectation is consistent with the fact that the apparent molecular surface tension of the hydration shell around a short *n*-alkane chain, obtained by dividing ΔG/SASA, is much smaller than the macroscopic air−water and oil−water surface tensions, as shown in Figure 5.[37] Moreover, these results also indicate that while the effective molecular surface tension of extended (all-trans) *n*-alkanes is expected to be slightly positive, that of flexible *n*-alkanes decreases with increasing chain length, again pointing toward a hydrophilic crossover. More specifically, a linear extrapolation of the molecular interfacial surface tension of flexible *n*-alkanes implies a hydrophobic crossover near C50. It is also interesting to note that although the magnitude of the molecular surface tension depends on the somewhat arbitrary use of SASA as the corresponding surface area, the predicted hydrophilic crossover is quite insensitive to this choice. For example, the crossover is predicted to occur at about the same chain length when molecular rather than solvent excluded surface areas of the alkanes are used to obtain molecular interfacial surface tensions. These predictions, combined with those shown in Figure 4, make it difficult to avoid the conclusion that the hydration free energies of long alkane chains are likely to be negative.

4. Discussion and Conclusions

A fundamental measure of hydropathy (illustrated in Figure 1) is used to predict the magnitude of the water-mediated collapse of *n*-alkane chains of various lengths. Recent simulations by Ferguson et al.[2] suggest that the water-mediated driving force for collapse only becomes significant for *n*-alkane chains longer than about C20. To establish physically reasonable bounds and predictions of the water-mediated driving force to fold longer chains, we have analyzed energetic and entropic contributions to the hydration of perfectly linear (all-trans) and collapsed (spherical) chain limits, as well as performed more detailed theoretical extrapolations of experimental and simulation results for flexible *n*-alkanes. Our results imply that the water-mediated free-energy change associated with the collapse of a C100 chain from a linear (all-trans) to a globular structure is of the order of −100 kJ/mol. This collapse free energy also implies that the resulting globular C100 chain should be hydrophilic, in the sense that its hydration free energy ΔG is predicted to be negative.

The physical basis for the predicted hydrophilic crossover can be traced to the relatively high density of methyl groups in a collapsed *n*-alkane chain. This methyl group density is nearly twice that at a macroscopic oil−water interface, and thus the cohesive van der Waals interaction energy between water and a collapsed *n*-alkane is expected to be significantly more negative than that at a macroscopic oil−water interface (per unit surface area). Moreover, recent nanoparticle hydration simulations by Chiu et al.[15] imply that a hydrophilic crossover can occur with increasing particle size, even in systems with a constant methyl group density. More specifically, the latter

interesting study reveals that the surface tension of such spherical nanoparticles should invariably decrease with decreasing surface curvature and thus can cross from positive (hydrophobic) to negative (hydrophilic) values with increasing particle size.

Accurately predicting the existence and location of the proposed hydrophilic crossover requires realistically accounting for differences between hydration of small *n*-alkanes, nanoscale chains, and macroscopic nonpolar interfaces. For example, if *n*-alkane hydration free energies were assumed to follow the simple linear solvent-accessible surface area (SASA) scaling of short chains, then no hydrophilic crossover would occur, and the resulting ΔG predictions would follow the dashed, all-trans line in Figure 4. While linear SASA scaling of small molecule ΔG values holds well,[38] there is every reason to expect that such scaling should not continue to realistically represent the hydration of nanoscale chains.[14,39,40] Our results suggest that E_{uv} values of both extended and collapsed *n*-alkanes up to about C100 do scale approximately linear their SASA value (as shown in Figure 4). However, TS_{uv} is not simply proportional to SASA, as indicated by the slightly nonlinear dependence of TS_{uv} on E_{uv} (see Figure 3). This dependence is consistent with the nonlinear chain length dependence of ΔG, whose negative curvature leads to the predicted hydrophilic crossover.

Although the solubility of paraffinic liquids or solids is certainly related to the ΔG value of an individual alkane chain, hydrophilic hydration (as defined by eq 1 and Figure 1) does not necessarily imply that solid paraffins should be highly soluble in water, as the solubility of paraffins is limited primarily by their very low equilibrium vapor pressures. Under ambient conditions, *n*-alkanes longer than C22 are solids whose vapor pressures become so low that they exceed current detection limits.[41] So, although long-chain *n*-alkanes may be hydrophilic with regard to the free energy of transferring a chain from the vapor phase to water, the solubility of the corresponding pure alkane liquid or solid is not expected to stray too far from the concentration associated with its equilibrium vapor pressure. On the other hand, our results imply that the collapse of an *n*-alkane chain in water should increase its solubility, and thus the solubility of large nonpolar solutes may be much higher than expected from a simple extrapolation of the experimental hydrophobicity of short-chain alkanes. For example, solubilities of spherical C60 Buckminsterfullerene nanoparticles are $\sim 10^{-11}$ M,[42] which is 30 orders of magnitude larger than would be predicted simply by extrapolating the experimental solubilities of short *n*-alkanes to a C60 *n*-alkane chain, $\sim 10^{-41}$ M. As another example, our estimates suggest that a C100 *n*-alkane chain may have a hydration free energy of the order of $\Delta G \sim -10$ kJ/mol. When compared with the $\Delta G = 90$ kJ/mol of an all-trans C100 chain, this suggests that a collapsed C100 may have a solubility as much as 18 orders of magnitude greater than an all-trans C100 chain. In other words, although the solubility of solid C100 paraffin is undoubtedly extremely low, it is likely to be significantly higher than one might have predicted from simple extrapolations of short-chain alkane results.

Our prediction that a hydrophilic crossover occurs upon the collapse of a long-chain alkane may seem to contradict the expectation that a hydrophilic polymer will expand rather than collapse in water. In fact, our results imply that a C100 *n*-alkane is very close to a hydropathic cusp, as it is hydrophobic when extended and slightly hydrophilic when collapsed. In other words, although water-mediated interactions are predicted to drive the hydrophobic collapse of a C100, the associated free energy decrease is predicted to be sufficiently large that the collapsed chain becomes slightly hydrophilic.

Although the solubilities of nanoscale synthetic polymers and proteins are undoubtedly strongly influenced by the presence of charged or electrostatic interactions, as well as hydrophobic side chains, the implications of a hydrophilic crossover for protein folding and other nanoscale hydration processes are potentially far-reaching. For example, recent protein folding studies highlight the interplay between side chain and backbone dynamics and in some cases suggest that the motions of the entire backbone dominate folding mechanisms.[43−45] Furthermore, recent protein folding simulations point to the need for refinement of potential functions to more accurately reproduce the experimental conformational structures and dynamics of proteins.[46,47] These results, combined with those of the present study, highlight the importance of the conformational degrees of freedom of macromolecular chains in accurately predicting and understanding biological and synthetic folding, binding, and self-assembly processes.

Appendix. Simulation Methods and Surface Tension Comparisons

Alkane−water interaction energies E_{uv} of *n*-alkane chains were obtained from isobaric−isothermal (NPT) molecular dynamics simulations performed using the simulation package GROMACS v. 3.3.[48] Approximately 4100 (for C20) to 60 000 (for C100) TIP4P waters[49] were used to hydrate the *n*-alkane chains, modeled using OPLS-AA potentials,[50] in a cubic box with periodic boundary conditions. The temperature and pressure of the system were maintained at 300 K and 1 atm with the Berendsen algorithm. A step size of 1 fs was used, and each simulation was run for 10 ns, after a 65 ps equilibration period. A cutoff of 0.9 nm was used for both the electrostatic and dispersive interactions in all simulations (increasing this cutoff did not significantly change our results, as further discussed below).

To generate E_{uv} values for all-trans chains, we maintained a rigid alkane conformation, using *x*, *y*, and *z* position restraints with a force of 10 000 kJ nm^{-1} mol^{-1} (while those for flexible *n*-alkanes were obtained without applying the latter constraint). Collapsed vapor phase conformations of a C100 chain were generated using a 100 ns NVT simulation of a single isolated chain. The hydration energies of several collapsed C100 structures selected from the latter equilibrated vapor phase simulation were obtained while holding the *n*-alkane conformation fixed.

The E_{uv} values obtained using a cutoff of 0.9 nm are within a few percent of those obtained using a longer potential cutoff (up to 1.25 nm) and/or Ewald treatment of long-range electrostatic interactions. The predicted hydrophilic crossover behavior is not significantly altered when the E_{uv} values of all the *n*-alkanes are changed by up to $\pm 10\%$ (and the TS_{uv} values are recalculated as described in Section 2).

The solvent accessible surface areas (SASA)[51] of *n*-alkane solutes were calculated with a carbon radius of 0.17 nm and hydrogen radius of 0.12 nm and a water probe radius of 0.14 nm.[31] Note that SASA is the surface area of the volume excluded to the center of the probe sphere (as it rolls over the solute surface). These SASA values were used both in generating Figure 4 and in estimating the apparent molecular surface tension results shown in Figure 5. The latter molecular surface tension is defined as the hydration free energy of a solute divided by its SASA and thus may be expressed in units of kilojoules per mol per square nanometer of solvent accessible surface area.

Note that surface tensions are often expressed in erg/cm^2 = mN/m, which may be converted to the latter units using 1 kJ/(mol nm^2) = 602.2 J/m^2 = 602.2 N/m.

References and Notes

(1) Lazaridis, T.; Karplus, M. *Biophys. Chem.* **2003**, *100* (1−3), 367–395.

(2) Ferguson, A. L.; Debenedetti, P. G.; Panagiotopoulos, A. Z. *J. Phys. Chem. B* **2009**, *113* (18), 6405–6414.

(3) Kauzmann, W. *Adv. Protein Chem.* **1959**, *14*, 1–63.

(4) Baysal, B. M.; Karasz, F. E. *Macromol. Theory Simul.* **2003**, *12* (9), 627–646.

(5) Pappu, R. V.; Wang, X.; Vitalis, A.; Crick, S. L. *Arch. Biochem. Biophys.* **2008**, *469* (1), 132–141.

(6) Gan, H. H.; Eu, B. C. *J. Chem. Phys.* **1998**, *109* (5), 2011–2022.

(7) Livadaru, L.; Kovalenko, A. *J. Chem. Phys.* **2004**, *121* (10), 4449–4452.

(8) Denesyuk, N. A.; Weeks, J. D. *Phys. Rev. Lett.* **2009**, *102* (10), 108101.

(9) Athawale, M. V.; Goel, G.; Ghosh, T.; Truskett, T. M.; Garde, S. *Proc. Natl. Acad. Sci. U.S.A.* **2007**, *104* (3), 733–738.

(10) ten Wolde, P. R.; Chandler, D. *Proc. Natl. Acad. Sci. U.S.A.* **2002**, *99* (10), 6539–6543.

(11) Dyson, H. J.; Wright, P. E.; Scheraga, H. A. *Proc. Natl. Acad. Sci. U.S.A.* **2006**, *103* (35), 13057–13061.

(12) Goel, G.; Athawale, M. V.; Garde, S.; Truskett, T. M. *J. Phys. Chem. B* **2008**, *112* (42), 13193–13196.

(13) Chandler, D. *Nature* **2005**, *437* (7059), 640–647.

(14) Lum, K.; Chandler, D.; Weeks, J. D. *J. Phys. Chem. B* **1999**, *103* (22), 4570–4577.

(15) Chiu, C. C.; Moore, P. B.; Shinoda, W.; Nielsen, S. O. *J. Chem. Phys.* **2009**, *131* (24), 244706.

(16) Ashbaugh, H. S.; Paulaitis, M. E. *J. Am. Chem. Soc.* **2001**, *123*, 10721.

(17) Acharya, H.; Vembanur, S.; Jamadagni, S. N.; Garde, S. *Faraday Discuss*. **2010**, 146, in press.

(18) Chakrabarty, S.; Bagchi, B. *J. Phys. Chem. B* **2009**, *113* (25), 8446–8448.

(19) Sutton, C.; Calder, J. A. *Proc. Natl. Acad. Sci. U.S.A.* **1974**, *8* (7), 654–657.

(20) Baker, E. G. *Science* **1959**, *129* (3353), 871–874.

(21) Franks, F. *Nature* **1966**, *210* (5031), 87–&.

(22) Peake, E.; Hodgson, G. W. *J. Am. Oil Chem. Soc.* **1967**, *44* (12), 696–&.

(23) Tolls, J.; van Dijk, J.; Verbruggen, E. J. M.; Hermens, J. L. M.; Loeprecht, B.; Schuurmann, G. *J. Phys. Chem. A* **2002**, *106* (11), 2760–2765.

(24) Ball, P. *Chem. Rev.* **2008**, *108* (1), 74–108.

(25) Tanford, C. *Science* **1978**, *200* (4345), 1012–1018.

(26) Poynor, A.; Hong, L.; Robinson, I. K.; Granick, S.; Zhang, Z.; Fenter, P. A. *Phys. Rev. Lett.* **2006**, *97* (26), 266101.

(27) Ben-Naim, A., *Solvation Thermodynamics*; New York: Plenum Press, 1987.

(28) Widom, B. *J. Phys. Chem.* **1982**, *86* (6), 869–872.

(29) Ben-Amotz, D.; Raineri, F. O.; Stell, G. *J. Phys. Chem. B* **2005**, *109* (14), 6866–6878.

(30) Ben-Amotz, D.; Underwood, R. *Acc. Chem. Res.* **2008**, *41* (8), 957–967.

(31) Bondi, A. *J. Phys. Chem.* **1964**, *68* (3), 441–&.

(32) Yaws, C. L. *Yaws' Handbook of Thermodynamic and Physical Properties of Chemical Compounds*; Knovel: Norwich, N. Y., 2003.

(33) Gallicchio, E.; Kubo, M. M.; Levy, R. M. *J. Phys. Chem. B* **2000**, *104* (26), 6271–6285.

(34) Ben-Amotz, D. *J. Chem. Phys.* **2005**, *123* (18), 184504.

(35) Levy, R. M.; Zhang, L. Y.; Gallicchio, E.; Felts, A. K. *J. Am. Chem. Soc.* **2003**, *125* (31), 9523–9530.

(36) Meyer, E. E.; Rosenberg, K. J.; Israelachvili, J. *Proc. Natl. Acad. Sci. U.S.A.* **2006**, *103* (43), 15739–15746.

(37) Tanford, C. *Proc. Natl. Acad. Sci. U.S.A.* **1979**, *76* (9), 4175–4176.

(38) Ashbaugh, H. S.; Kaler, E. W.; Paulaitis, M. E. *J. Am. Chem. Soc.* **1999**, *121* (39), 9243–9244.

(39) Konig, G.; Boresch, S. *J. Phys. Chem. B* **2009**, *113* (26), 8967–8974.

(40) Chen, J.; Brooks, C. L. *Phys. Chem. Chem. Phys.* **2008**, *10* (4), 471–481.

(41) Chickos, J. S.; Hanshaw, W. *J. Chem. Eng. Data* **2004**, *49* (1), 77–85.

(42) Jafvert, C. T.; Kulkarni, P. P. *Environ. Sci. Technol.* **2008**, *42* (16), 5945–5950.

(43) Wei, Y. J.; Nadler, W.; Hansmann, U. H. E. *J. Chem. Phys.* **2006**, *125* (16), 164902.

(44) Tran, H. T.; Mao, A.; Pappu, R. V. *J. Am. Chem. Soc.* **2008**, *130* (23), 7380–7392.

(45) Sinha, K. K.; Udgaonkar, J. B. *Curr. Sci.* **2009**, *96* (8), 1053–1070.

(46) Freddolino, P. L.; Park, S.; Roux, B.; Schulten, K. *Biophys. J.* **2009**, *96* (9), 3772–3780.

(47) Meinke, J. H.; Hansmann, U. H. E. *J. Comput. Chem.* **2009**, *30* (11), 1642–1648.

(48) Lindahl, E.; Hess, B.; van der Spoel, D. *J. Mol. Model.* **2001**, *7* (8), 306–317.

(49) Jorgensen, W. L.; Chandrasekhar, J.; Madura, J. D.; Impey, R. W.; Klein, M. L. *J. Chem. Phys.* **1983**, *79* (2), 926–935.

(50) Jorgensen, W. L.; Maxwell, D. S.; TiradoRives, J. *J. Am. Chem. Soc.* **1996**, *118* (45), 11225–11236.

(51) Eisenhaber, F.; Lijnzaad, P.; Argos, P.; Sander, C.; Scharf, M. *J. Comput. Chem.* **1995**, *16* (3), 273–284.

JP912089Q